



Contents List available at JACS Directory

Journal of Advanced Chemical Sciences

journal homepage: www.jacsdirectory.com/jacs

Inhibition of Substituted Thiadiazole Derivatives for the Control of Corrosion of Copper-Nickel (70/30) Alloy in Sea Water

N. Balamurugapandian¹, R. Ravichandran^{2,*}¹Research and Development Centre, Bharathiar University, Coimbatore – 641 046, Tamil Nadu, India.²Post Graduate and Research Department of Chemistry, Dr. Ambedkar Government Arts College (Autonomous), Chennai – 600 039, Tamil Nadu, India.

ARTICLE DETAILS

Article history:

Received 10 October 2016

Accepted 15 November 2016

Available online 25 November 2016

Keywords:

Copper-Nickel Alloy

Thiadiazole

Natural Seawater

Impedance

Adsorption Isotherm

ABSTRACT

Inhibitive action of four thiadiazole derivatives namely 2-amino-5-methyl-1, 3, 4-thiadiazole (AMTD), 2-amino-5-methylthio-1, 3, 4-thiadiazole (ATTD), 2-amino-5-(4-tert-butyl)-1, 3, 4-thiadiazole (ABTD), 2-amino-5-(4-ethylphenyl)-1, 3, 4-thiadiazole (AETD) on the corrosion of copper-nickel alloy in natural sea water has been studied. Mass loss, polarisation and impedance measurements have been employed to analyse their inhibition behavior of substituted thiadiazole derivatives. Polarization measurements showed that the thiadiazoles inhibits the corrosion of copper-nickel alloy by blocking the active sites of the metal surface. Impedance parameters such as charge transfer resistance (R_{ct}) and double layer capacitance (C_{dl}) are related to adsorption of inhibitors on the metal surface, leading to the formation of a protective film. The adsorption of thiadiazole derivatives on the alloy surface in natural seawater obeys the Langmuir adsorption isotherm.

1. Introduction

Copper is one of the most commonly used metals that have extensive applications in various industrial processes [1]. Copper-based alloys have a long history of service in marine environments. In general, they exhibit an attractive combination of properties, e.g., good machinability, good resistance to corrosion and bio-fouling and superior thermal and electrical conductivities [2, 3]. In view of their good machinability, they are available in a wide range of products [4]. The 70/30 copper-nickel alloy is a material of selection for condensers and heat exchangers, where seawater is used as a coolant and in desalination plants. This alloy is resistant to stress corrosion cracking by ammonia and sulphide ions [5] and has good resistance to bio-fouling due to the release of copper ions [6, 7]. This alloy is also resistant to pitting and crevice corrosion in quiet seawater [8]. The corrosion resistance of this alloy is related to the performance of the passive film, which is mainly composed of Cu_2O [9-11]. The cupric species generally overlies the cuprous species. However, in the sulphide containing seawater, the corrosion rate of Cu-Ni (90/10) alloy is increased as the sulphide ions interfere with the film formation and produce a non-protective black layer containing cuprous oxide and sulphide ions [12]. The pollution of seawater with sulphide ions at the coastal areas can occur due to industrial waste water discharges into sea and also due to biological and bacteriological processes taking place in seawater. Thus, corrosion of Cu-Ni alloy in seawater polluted with sulphide ions is a serious problem, which has drawn the attention of the researchers in this field.

One of the most important methods in corrosion protection is the utilisation of organic inhibitors. Many mechanisms have been proposed for the inhibition of metal corrosion by organic inhibitors which takes place via adsorption on the metal surface [13, 14]. The adsorption process leads to an effective blocking of the active sites of metal dissolution and/or hydrogen evolution, which results in a considerable decrease in the corrosion rate. Numerous heterocyclic compounds containing nitrogen have been examined for use as inhibitors for its corrosion. Benzotriazole proved to be the most effective class of inhibitors for copper and copper base alloys in many aqueous environments [15]. Badawy et al. [16] studied the corrosion inhibition of Cu-5Ni and Cu-65Ni alloys in 0.6 moldm^{-3}

chloride solution using amino acids as inhibitors. Benmessouad et al. [17] studied the inhibiting effect of 2-mercaptobenzimidazole against the corrosion of 70Cu-30Ni alloy in aerated 3% sodium chloride solution polluted with ammonia (pH = 9.25) by potentiodynamic polarization studies and electrochemical impedance studies. 1,2,3-benzotriazole is a well-known corrosion inhibitor for copper. Frignani et al. [18] investigated the influence of alkyl chain on the protective effects of benzotriazole towards copper in acidic chloride solution. Qafsaoui et al. [19] also reported that the growth of protective film on copper in the presence triazole derivatives. Shukla and Pitre [20] studied the electrochemical behavior of brass and the inhibitive effect of imidazole in acid solution. Mernari et al. [21] investigated the inhibitive effects of 3,5-bis(N-pyridyl)4-amino-1,2,4-triazoles on the corrosion of mild steel in 1 M hydrochloric acid.

2. Experimental Methods

2.1 Materials

The material used for this study was copper-nickel alloy supplied in the form of sheet and the composition is given in Table 1. The natural sea water was collected near National Thermal Power Corporation (NTPC), Ennore, Chennai, India and the chemical composition of the seawater was given in Table 2. The pH of the seawater is 6.5. The inhibitors thiadiazole derivatives (Sigma-Aldrich) and absolute ethanol (Merck) were used as received. The structures of thiadiazole derivatives are shown in Fig. 1.

Table 1 Chemical composition of Cu/Ni (70/30) (in wt%)

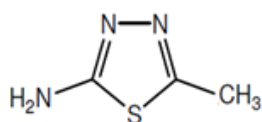
Alloy	Cu	Ni	Fe	Sn	Pb	Al	Mn, As, Co, Sr
Composition	69.78	29.43	0.18	0.06	0.09	0.28	0.0551

Table 2 Composition of natural seawater

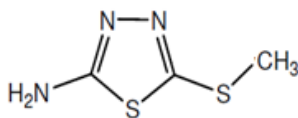
Species	Cl ⁻	SO ₄ ²⁻	S ²⁻	HCO ₃ ⁻	PO ₄ ³⁻	CO ₃ ²⁻	NO ₂ ⁻	NO ₃ ⁻	Br ⁻	F ⁻
Concentration (g/L)	35.24	4.56	2.49	0.94	2.12	1.28	0.24	0.31	0.32	0.04

*Corresponding Author

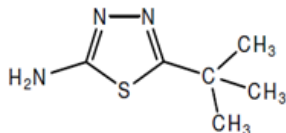
Email Address: varmaravi1965@rediffmail.com (R. Ravichandran)



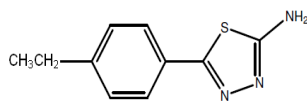
2-amino-5-methyl-1,3,4-thiadiazole (AMTD)



2-amino-5-methylthio-1,3,4-thiadiazole (ATTD)



2-amino-5-(4-tert-butyl)-1,3,4-thiadiazole (ABTD)



2-amino-5-(4-ethylphenyl)-1,3,4-thiadiazole (AETD)

Fig. 1 Structures of Thiadiazole Derivatives

2.2 Methods

For mass-loss method, the copper-nickel alloy specimens (4 cm x 2.5 cm x 0.2 cm) were abraded with silicon carbide papers (120-1200 grit), thoroughly washed with distilled water, degreased with acetone, rinsed with distilled water, dried and weighed. The specimens were immersed in 300 mL of natural seawater, with and without inhibitors at 30 °C for 30 days.

For electrochemical studies, the working electrode with an area of 1 cm² was embedded in epoxy resin in a Teflon holder. The electrode was abraded mechanically with silicon carbide papers from 120 to 1200 grit followed by polishing with 5 μm diamond paste. The electrode was thoroughly washed with double distilled water, degreased in acetone for 15 minutes using ultrasonic vibration, rinsed with distilled water and dried. The cell assembly consisted of copper-nickel alloy as working electrode, a platinum foil as counter electrode and a saturated calomel electrode (SCE) as a reference electrode with a Luggin capillary bridge.

Polarization studies were carried out using an Electrochemical workstation (Model: CHI 760C, CH instruments, USA) at a scan rate of 1 mV/s. The working electrode was immersed in natural sea water (open atmosphere) and allowed to stabilize for 30 minutes [22]. In each case a potential of -1.5 V was then applied for 15 minutes to reduce oxides. The cathodic and anodic polarization curves for copper-nickel alloy specimen in the test solution with and without inhibitors were recorded between -500 to 500 mV at a scan rate of 1 mV/s at a temperature range from 303 K to 343 K. The inhibition efficiencies of the compounds were determined from corrosion current density using the Tafel extrapolation method. A.C. impedance measurements were conducted at room temperature using an AUTOLAB with Frequency Response Analyzer (FRA), which included a Potentiostatic model "Autolab PGSTAT 12. An ac sinusoid of ±10 mV was applied at the corrosion potential (E_{corr}). The frequency range of 100 kHz to 1 MHz was employed. All potentials are reported vs. SCE.

3. Results and Discussion

3.1 Mass Loss Method

The average mass loss data obtained for the copper-nickel alloy specimen in triplicates for various concentrations of thiadiazole derivatives are listed in Table 3. From the mass loss data, it is clear that the mass loss of alloy specimens decreases with increasing the inhibitor concentration. Furthermore, it is found that the corrosion rate is linearly proportional to the mass loss. This means that the corrosion rate decreases with the increase in concentration of the inhibitors, as listed in Table 3. The results indicate that, the mass loss of alloy sample decreases when compared with the absence of thiadiazole derivatives (inhibitors), because, the thiadiazole forms a preventive layer on the metal surface. Hence, for this inhibitor, the inhibition efficiency (IE) also increases with the increase of concentration. The degrees of surface coverage (θ) for different concentrations of inhibitor have been evaluated from the mass

loss method. This is due to the following reason. For this inhibitor, the surface coverage increases with the increase of concentration and reaches a limiting value at a higher inhibitor concentration. Correlation between θ values and inhibition efficiency suggests that the inhibitive action is through adsorption. From these experimental studies, it is clear that, thiadiazole derivatives act as good inhibitor. The results of this study confirm that whenever two or more hetero atoms or electro active groups are present, the inhibition nature of compound is enhanced. This interaction favours the adsorption and film formation on the surface.

Table 3 Mass loss measurements of copper-nickel alloy at different concentrations of AMTD, ATTD, ABTD and AETD in natural sea water

Inhibitor concentration (ppm)	Mass loss (mg)	Corrosion rate x 10 ⁻² (mmpy)	Degree of surface coverage (θ) (%)	Inhibition efficiency (%)
Blank	123.12	13.46	-	-
AMTD				
10 ⁻⁵	65.47	7.26	0.4682	46.82
10 ⁻⁴	43.78	4.95	0.6451	64.51
10 ⁻³	17.85	2.13	0.8550	85.50
10 ⁻²	18.13	2.14	0.8527	85.27
ATTD				
10 ⁻⁵	58.45	6.52	0.5253	52.53
10 ⁻⁴	37.37	4.13	0.6965	69.65
10 ⁻³	11.78	1.94	0.9043	90.43
10 ⁻²	12.04	1.96	0.9022	90.22
ABTD				
10 ⁻⁵	49.91	5.45	0.5946	59.46
10 ⁻⁴	31.06	3.64	0.7477	74.77
10 ⁻³	07.24	1.26	0.9412	94.12
10 ⁻²	07.51	1.29	0.9390	93.90
AETD				
10 ⁻⁵	44.62	5.08	0.6376	63.76
10 ⁻⁴	21.91	2.89	0.8220	82.20
10 ⁻³	3.43	1.03	0.9721	97.21
10 ⁻²	3.52	1.07	0.9714	97.14

3.2 Polarization Studies

The cathodic and anodic polarization curves of copper-nickel alloy in natural sea water with optimum concentrations of AMTD, ATTD, ABTD and AETD are shown in Fig. 2. It is evident that, in the presence of inhibitor, the cathodic and anodic curves were shifted and the shift was found to be dependent on inhibitor concentration. Table 4 illustrates the corresponding electrochemical parameters. The E_{corr} values were marginally shifted in the presence of AMTD, ATTD, ABTD and AETD. This observation clearly indicated that the inhibitors control the anodic and cathodic reactions and thus act as mixed-type inhibitors. The current density also decreased with increasing concentration of the inhibitors. The inhibition efficiency was calculated from I_{corr} values.

Table 4 Tafel polarization parameters for the corrosion of cupro-nickel alloy in natural seawater at different concentrations of AMTD, ATTD, ABTD and AETD

Inhibitor concentration (ppm)	I_{corr} (μAcm^{-2})	$-E_{\text{corr}}$ (mV vs. SCE)	β_a	β_c	Corrosion rate x 10 ⁻² (mmpy)	Inhibition efficiency (%)
Blank	9.93	202	53	-132	12.53	-
AMTD						
10 ⁻⁵	5.38	219	65	-97	6.79	45.81
10 ⁻⁴	3.69	220	82	-86	4.66	62.81
10 ⁻³	1.71	239	104	-63	2.16	82.76
10 ⁻²	1.72	221	112	-56	2.17	82.68
ATTD						
10 ⁻⁵	5.11	214	72	-92	6.45	48.52
10 ⁻⁴	3.47	222	87	-76	4.38	65.04
10 ⁻³	1.42	236	110	-54	1.79	85.71
10 ⁻²	1.44	234	119	-45	1.82	85.47
ABTD						
10 ⁻⁵	4.63	216	75	-88	5.84	53.39
10 ⁻⁴	2.99	221	89	-71	3.77	69.91
10 ⁻³	1.12	234	115	-50	1.41	88.75
10 ⁻²	1.13	230	125	-41	1.43	88.59
AETD						
10 ⁻⁵	4.35	215	79	-80	5.49	56.19
10 ⁻⁴	2.82	223	94	-65	3.56	71.59
10 ⁻³	0.94	241	122	-46	1.19	90.50
10 ⁻²	0.95	232	128	-36	1.20	90.42

The values of cathodic Tafel slope (β_c) and anodic Tafel slope (β_a) of thiadiazole derivatives were found to change with inhibitor concentration, which clearly indicates that the inhibitors controlled both the reactions. The inhibition efficiency of AMTD, ATTD, ABTD and AETD in natural sea water attained a maximum value of 82.76%, 85.71%, 88.75 and 90.50% at 10^{-3} M concentration respectively. The values of inhibition efficiency increase with increasing concentration of inhibitor, indicating that a higher surface coverage was obtained in a solution with the optimum concentration of inhibitor [23]. The corrosion rate of copper-nickel alloy in natural sea water was found to be 12.53×10^{-2} mmpy and it was minimized by adding the inhibitors to a lower value of 2.16×10^{-2} mmpy, 1.79×10^{-2} mmpy, 1.41 mmpy and 1.19×10^{-2} mmpy for copper-nickel alloy due to the adsorption of AMTD, ATTD, ABTD and AETD on the metal surface respectively.

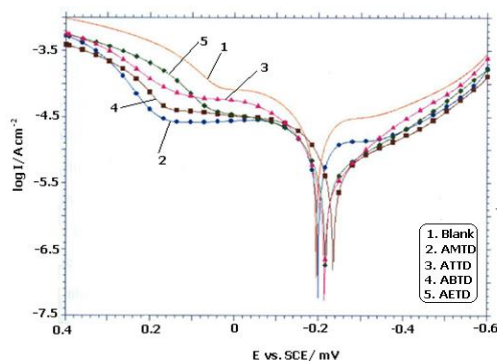


Fig. 2 Tafel Polarization curves of copper-nickel alloy in natural sea water containing optimum concentrations of AMTD, ATTD, ABTD and AETD

3.3 Electrochemical Impedance Spectroscopic Studies

Electrochemical impedance spectroscopic technique is a powerful tool in the investigation of the corrosion and adsorption phenomena. This method explains effectively the corrosion and passivation phenomena of metals and alloys. The impedance diagrams represented in Nyquist plot obtained at open-circuit potential after one hour immersion in natural seawater in the presence and absence of thiadiazole derivatives are presented in Fig. 3. The percent inhibition efficiency (IE %) of copper-nickel was calculated as follows [24]:

$$IE \% = \frac{(R_{ct})^{-1} - (R_{ct(inh)})^{-1}}{(R_{ct})^{-1}} \times 100$$

where, $R_{ct(inh)}$ and R_{ct} are the charge-transfer resistance values with and without inhibitors respectively.

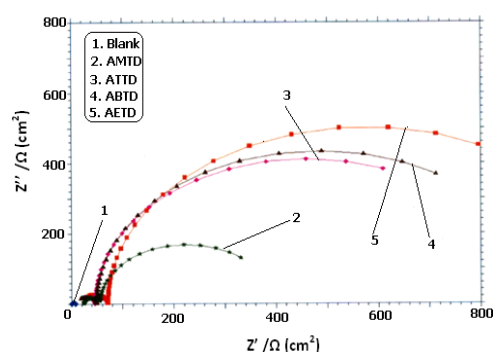


Fig. 3 Nyquist diagram of cupro-nickel alloy in natural sea water containing optimum concentration of thiadiazole derivatives

The calculated parameters obtained from equivalent circuit fitting analysis in the absence and presences of inhibitors in natural seawater are given in Table 5. Nyquist plots obtained for the alloy in the presence of different concentrations of inhibitor exhibited different shapes, which indicated the change in corrosion mechanism due to the presence of inhibitors. It can be seen from the table that with increase in inhibitor concentration, R_{ct} value increased and C_{dl} value decreased. The decrease in C_{dl} value can result from a decrease in local dielectric constant and/or an increase in the thickness of the electrical double layer, suggests that, the thiadiazole derivatives function by adsorption at the metal-solution interface. The decrease in C_{dl} value upon increase in inhibitor concentration was due to reduced access of charged species to the alloy

surface, as inhibitor has adsorbed and a good persistent layer of the same was formed on the alloy surface. The change in R_{ct} and C_{dl} values was caused by the gradual replacement of water molecules by the anions of the NaCl present in seawater and adsorption of the organic inhibitor molecules on the metal surface, reducing the extent of dissolution. The value of Faradic resistance (R_F) increases with increase in concentration showing that AMTD, ATTD, ABTD and AETD stabilize the corrosion products on the metal surface. As the concentration of the inhibitor increases, the inhibitors get adsorbed effectively on the alloy surface which increases the R_F values and decreases the C_F values.

The molecular structure normally determines the type of adsorption on copper-nickel surface. Thiadiazole derivatives viz., AMTD, ATTD, ABTD and AETD show differences in their inhibition efficiency due to the difference in their molecular structures. Of the thiadiazole derivatives studied, AETD has the highest inhibition efficiency and this corresponds well with the polarization measurements. The % IE calculated from EIS shows the same trend as those estimated from polarization measurements i.e., polarization measurements and EIS study complement each other well.

Table 5 Electrochemical impedance data of copper-nickel alloy in natural Seawater containing different concentrations of AMTD, ATTD, ABTD and AETD

Inhibitor concentration (ppm)	$R_{ct} \times 10^4$ (Ωcm^2)	C_{dl} (μFcm^{-2})	$R_F \times 10^4$ (Ωcm^2)	C_F (μFcm^{-2})	IE (%)
Blank	0.58	77.45	0.65	90.34	-
AMTD					
10^{-5}	2.52	09.82	2.72	14.32	71.12
10^{-4}	5.97	1.27	4.52	5.21	82.26
10^{-3}	16.34	0.41	15.39	1.46	93.84
ATTD					
10^{-5}	3.68	6.56	2.86	13.97	73.66
10^{-4}	6.59	1.12	5.67	4.21	85.28
10^{-3}	18.48	0.29	15.46	1.32	95.13
ABTD					
10^{-5}	4.44	5.84	3.35	11.12	75.22
10^{-4}	7.83	0.91	5.86	2.83	87.93
10^{-3}	19.78	0.13	19.84	1.02	96.85
AETD					
10^{-5}	5.21	2.78	5.75	11.78	78.43
10^{-4}	9.97	0.64	10.87	2.39	90.26
10^{-3}	22.75	0.02	25.96	0.63	97.94

3.4 Effect of Temperature

To gain insight into the nature of adsorption, the effect of temperature on the corrosion behavior of copper-nickel alloy in natural seawater was studied. The temperature can modify the interaction between the electrode and the seawater media. The effect of temperature on the rate of dissolution of copper-nickel alloy in natural seawater containing optimum concentration (10^{-3} M) of the investigated inhibitors was tested by polarization method over a temperature range from 303 to 333 K and the corrosion parameters and inhibition efficiencies are given in Table 6. These results revealed that on increasing the temperature, there is an increase in corrosion current density as well as corrosion rate for uninhibited and inhibited solutions.

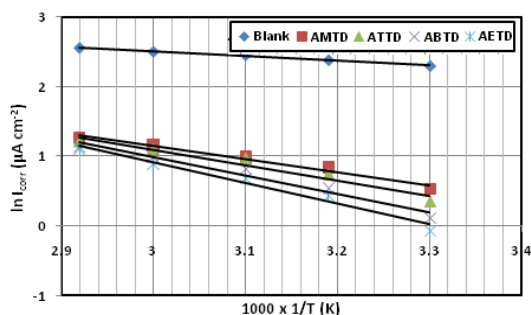
The dependence of the corrosion rate on temperature can be expressed by the Arrhenius equation, since the corrosion reaction can be regarded as Arrhenius type process. The activation parameters can be calculated using the Arrhenius equation:

$$I_{\text{corr}} = A \exp(-E_a / RT)$$

where the pre-exponential factor A is the adsorption constant, R is the universal gas constant, T is the absolute temperature and E_a is the activation energy of the corrosion process. Plotting the natural logarithm of the corrosion current density against $1/T$, the activation energies in the absence and presence of optimum concentration were calculated from the slope. Fig. 4 shows the Arrhenius plots for copper-nickel alloy in seawater in the absence and presence of 10^{-3} M concentration of AMTD, ATTD, ABTD and AETD at different temperatures. For instance, the activation energy for the blank was found to be 12.98 kJmol^{-1} . However in the presence of AMTD, ATTD, ABTD and AETD, the activation energies were 35.83 kJmol^{-1} , 42.46 kJmol^{-1} , 51.47 kJmol^{-1} and 59.83 kJmol^{-1} respectively. It is clear that the activation energy values obtained in the presence of inhibitors are higher than that obtained in the absence of inhibitor, indicating that the addition of inhibitors enhances corrosion resistance of the alloy. The increase in activation energy after the addition of the inhibitor into the seawater indicates that physical adsorption (electrostatic) occurs initially.

Table 6 Polarisation parameters of copper-nickel alloy in natural seawater containing optimum concentration of thiadiazole derivatives at temperature range from 303 K– 343 K

Inhibitor	Temp (K)	$E_{corr}/mV_{vs.SCE}$	$I_{corr}/\mu A cm^{-2}$	$\beta_a (mVdec^{-1})$	$\beta_c (mVdec^{-1})$	CR (mmpy)	IE (%)
Blank	303	187	9.93	69	-121	12.53	-
	313	169	10.82	58	-128	13.65	-
	323	158	11.56	52	-134	14.59	-
	333	151	12.18	39	-143	15.37	-
	343	138	12.84	33	-151	16.20	-
AMTD	303	268	1.71	132	-57	2.16	82.76
	313	261	2.31	129	-63	2.92	78.65
	323	252	2.68	121	-73	3.38	76.82
	333	244	3.19	118	-78	4.03	73.81
	343	231	3.51	112	-82	4.43	72.66
ATTD	303	262	1.42	138	-52	1.79	85.71
	313	249	2.09	133	-55	2.64	75.60
	323	242	2.63	127	-60	3.32	77.25
	333	227	2.96	122	-68	3.74	75.70
	343	216	3.35	114	-76	4.23	73.91
ABTD	303	255	1.12	145	-50	1.41	88.75
	313	244	1.72	141	-53	2.17	84.10
	323	232	2.26	133	-59	2.85	80.45
	333	224	2.69	129	-64	3.39	77.91
	343	216	3.13	117	-73	3.95	75.62
AETD	303	236	0.94	148	-43	1.19	90.50
	313	217	1.56	143	-48	1.97	85.58
	323	204	1.99	137	-55	2.51	82.79
	333	183	2.43	130	-61	3.07	80.04
	343	177	2.94	123	-69	3.71	77.10

**Fig. 4** Arrhenius plots for the copper-nickel alloy in natural sea water containing optimum concentration of thiadiazole derivatives

The higher E_a value for the copper-nickel alloy in the inhibited solution can be correlated with the increased stability of the film formed, which enhances the activation energy of the corrosion process. Generally an increase in temperature usually accelerates corrosive processes, giving rise to higher metal dissolution rates and a possible shift of the adsorption-desorption equilibrium towards desorption. This, as well as roughening of the metal surface as a result of enhanced corrosion, may also reduce the adsorption ability of the inhibitor on the metal surface. The increase in solution temperature slightly shifts E_{corr} values and enhances both cathodic and anodic current densities. The decrease in inhibition efficiency with increasing temperature may be due to the increase in desorption of inhibitors followed by dissolution of copper and nickel.

3.5 Adsorption Isotherm and Thermodynamic Parameters

It is generally assumed that the adsorption of inhibitors on the metal surface is the essential step in the mechanism of inhibition. Adsorption isotherms are very important in understanding the mechanism of organo electrochemical reactions. The most frequently used isotherm are Langmuir, Frumkin, Hill de-Boer, Parsons, Temkin, Flory-Huggins and Freundlich. Basic information on the interaction between the inhibitor and the copper-nickel alloy surface can be provided by the adsorption isotherm and in general the inhibitors can function either by physical (electrostatic) adsorption or chemisorptions on the metal. To obtain more information about the interaction between the studied inhibitor systems with alloy surface, different adsorption isotherms were used. For organic inhibitors that have the ability to adsorb strongly on metal surface, the adsorption behavior of the organic substrate on the metal surface must be known. The fractional surface coverage of θ of AMTD, ATTD, ABTD and AETD in seawater medium at the temperature range of 303–343 K was

determined from the potentiodynamic polarization measurements data using the formulas.

$$\theta = \frac{I_{corr} - I_{corr(inh)}}{I_{corr}} \quad (1)$$

where, I_{corr} and $I_{corr(inh)}$ are the values of corrosion current density of uninhibited and inhibited systems respectively.

$$Kc = \frac{\theta}{1-\theta} \quad (2)$$

where, c is the concentration of the inhibitor and θ is the fractional surface coverage. The Langmuir isotherm Eq. (2), which is based on the assumption that all adsorption sites are equivalent and molecular binding, occurs independently from the fact that, whether the nearby sites are occupied or not, was verified for all the studied inhibitors. The adsorption equilibrium constant K is related to the free energy of adsorption ΔG_{ads} as

$$K = \frac{1}{C_{solvent}} \exp \left[\frac{\Delta G_{ads}}{RT} \right] \quad (3)$$

where, $C_{solvent}$ represents the molar concentration of the solvent, which in the case of water is 55.5 mol dm^{-3} , R is the universal gas constant and T is the absolute temperature in K. The Langmuir isotherm, Eq. (2) can be rearranged to obtain the following expression,

$$\frac{c}{\theta} = \frac{1}{K} + c \quad (4)$$

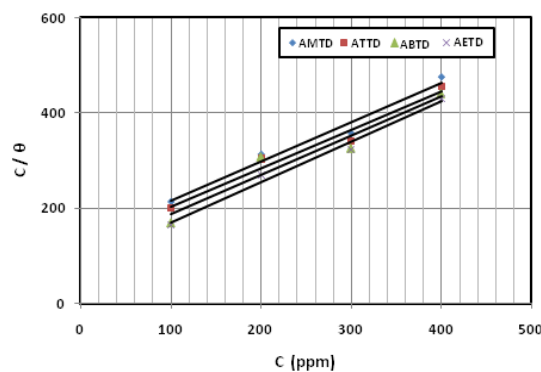
So that a linear relationship can be obtained on plotting $\frac{c}{\theta}$ as a function of c , with a slope of unity.

The high value of the adsorption equilibrium constant reflects the high adsorption ability of these inhibitors on the alloy surface. A plot of C_{inh}/θ against C_{inh} shows a straight line indicating that adsorption follows the Langmuir adsorption isotherm as shown in Fig. 5.

The standard equilibrium constant of adsorption K_{ads} and the free energy of adsorption (ΔG_{ads}) are related to the following equation,

$$\Delta G_{ads} = -2.303 RT \log(55.5K_{ads}) \quad (5)$$

where, R is the universal gas constant, T is the absolute temperature and the molar concentration of water per litre is 55.5.

**Fig. 5** Langmuir adsorption isotherm plot for the copper-nickel alloy in natural sea water containing different concentration of thiadiazole derivatives

Thermodynamic parameters including heat of adsorption, free energy of adsorption and the entropy of adsorption are important in the explanation of the corrosion inhibition mechanism. The thermodynamic parameters obtained are given in Table 7. It can be seen from the table that K_{ads} decreases with increase in temperature which indicates a decrease in the extent of adsorption of inhibitor molecules on copper-nickel alloy. It is also indicated that the interactions between the adsorbed molecules and the metal surface are weakened and, consequently, the adsorbed molecules become easily removable [25]. The negative value of ΔG_{ads} indicates spontaneous adsorption of the AMTD, ATTD, ABTD and AETD on the alloy surface and also the strong interaction between inhibitor molecules and the metal surface.

It is generally accepted that the values of ΔG_{ads} up to -20 kJ mol^{-1} are consistent with the electrostatic interactions between the charged molecules and the charged metal (physisorption) while those around -40 kJ mol^{-1} or higher associated with chemisorption as a result of sharing or transfer of electrons from organic molecules to the metal surface to form a coordinate type of bond. The values of ΔG_{ads} in the above measurements was more than -20 kJ mol^{-1} suggested that AMTD, ATTD, ABTD and AETD

at 10^{-2} M are chemisorbed on the alloy surface. It may be assumed that adsorption occurs first due to the strong adsorption of water molecules on the surface of alloy. The chemical interaction between metal surface and the organic molecules followed by the removal of water molecules from the surface turns to be chemisorption [26].

Table 7 Thermodynamic parameters for the adsorption of thiadiazole derivatives on the alloy surface in natural seawater at different temperatures

Inhibitors	Temp (K)	K_{ads} dm^3mol^{-1}	$-\Delta G_{ads}$ $(KJmol^{-1})$	$-\Delta H_{ads}$ $(KJmol^{-1})$	$-\Delta S$ $(Jmol^{-1}K^{-1})$
AMTD	303	2955	30.26	42.38	39.08
	313	2302	30.60	42.38	37.64
	323	2071	31.30	42.38	34.30
	333	1761	31.81	42.38	31.74
	343	1660	32.60	42.38	28.51
ATTD	303	4997	31.57	43.98	40.96
	313	2581	30.90	43.98	41.79
	323	2829	32.13	43.98	36.68
	333	2596	32.89	43.98	33.30
	343	2360	33.60	43.98	30.26
ABTD	303	7178	32.48	47.36	49.19
	313	4808	32.51	47.36	47.44
	323	3740	32.88	47.36	44.83
	333	3206	33.47	47.36	41.71
	343	2819	34.12	47.36	38.60
AETD	303	9526	33.20	51.72	61.12
	313	5934	33.06	51.72	59.61
	323	4810	33.56	51.72	56.22
	333	4010	34.09	51.72	52.94
	343	5269	34.61	51.72	49.88

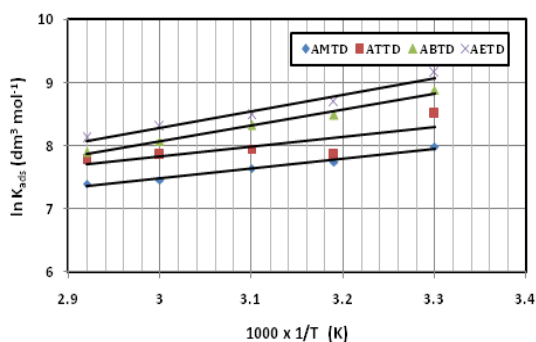


Fig. 6 Adsorption isotherm plot for thiadiazole derivatives in natural sea water

The negative ΔG values indicate the spontaneity of the adsorption of studied inhibitors on brass in the temperature range from 303 to 343 K. It is known that the ΔG values indicate the chemisorption mode. As the temperature increases, the value of free energy of adsorption decreases negatively indicating desorption of the studied inhibitors. It is observed that a limited decrease in the absolute value of ΔG with increase in temperature, indicating that adsorption is unfavorable with increasing temperature and that both physisorption and chemisorption have equal contribution in the adsorption mechanism. ΔH is another criterion from which the mode of adsorption can be proved based on the absolute value. The amount of heat of adsorption (ΔH) can be calculated using the following equation:

$$\ln K_{ads} = \left(-\frac{\Delta H}{RT}\right) + \text{constant} \quad (6)$$

Plot of $\ln K_{ads}$ versus $1/T$ at the optimum concentration (300 ppm) is shown in Fig. 6 to calculate the heat of adsorption. The straight lines were obtained with slope equal to $(-\Delta H_{ads}/RT)$.

Generally an endothermic process is explicit to chemisorption while an exothermic adsorption process designates either physisorption or chemisorption. In an exothermic adsorption, the adsorption mode is judged based on the absolute value of ΔH . Enthalpy of adsorption of absolute values lower than 40 kJmol^{-1} indicates physisorption and values approaching 100 kJmol^{-1} indicate chemisorptions [27]. It is evident from the table that the adsorption is an exothermic process. In our case, the absolute values of enthalpy of the studied inhibitors are higher than 40 kJmol^{-1} confirming chemisorption.

Entropy of inhibitor adsorption (ΔS) can be calculated using the following equation:

$$\Delta G_{ads} = \Delta H_{ads} - T\Delta S_{ads} \quad (7)$$

The negative values of ΔS_{ads} in the adsorption process can be explained as; inhibitor molecules are adsorbed in orderly fashion onto the brass surface, causing a decrease in entropy.

The negative values of ΔS_{ads} are expected as the adsorption process which is accompanied by a decrease in the disorder of the system due to the adsorption of the free thiadiazole derivatives onto the alloy surface. Therefore negative values of ΔS_{ads} in the present investigation support the higher absorbability of organic compounds on the metal surface.

4. Conclusion

Thiadiazole derivatives AMTD, ATTD, ABTD and AETD show good inhibition efficiency in natural sea water. AETD exhibits highest inhibition efficiency. The polarization data indicate that the corrosion rate increases and inhibition efficiency decreases with increase of temperature. The decrease of inhibition efficiency with increase in temperature observed in the presence of the optimum concentrations of thiadiazole derivatives proved that their protective effectiveness on copper-nickel alloy corrosion is temperature-dependent. The inhibitors easily adsorb on the alloy surface at the corrosion potential and form a protective complex with the Cu (I) ion, controlling copper-nickel alloy from corrosion. Electrochemical impedance spectroscopy shows that R_{ct} values increase, while C_{dl} values decrease in the presence of thiadiazole derivatives. The low C_{dl} value obtained in the presence of inhibitors indicate the formation of thicker inhibitor film on the metal surface. The studied inhibitors are found to follow the Langmuir's adsorption isotherm, indicating that the inhibition process occurs via adsorption. The high value of adsorption equilibrium constant (K_{ads}) suggested that the inhibitors are strongly adsorbed on the alloy surface. The negative values of the ΔG_{ads} and ΔH_{ads} indicated that the adsorption process was spontaneous and exothermic.

References

- [1] M.M. El-Naggar, Bis-triazole as a new corrosion inhibitor for copper in sulfate solution, A model for synergistic inhibition action, J. Mater. Sci. 35 (2000) 6189-6195.
- [2] R. Gasparac, C.R. Martin, E. Stupnisek-Lisac, Z. Mandic, In-situ studies of imidazole and its derivatives as copper corrosion inhibitors, J. Electrochem. Soc. 147 (2000) 548-551.
- [3] A. Naguib, F. Mansfeld, Evaluation of corrosion inhibition of brass in chloride media using EIS and ENA, Corros. Sci. 43 (2001) 2147-2171.
- [4] C.A. Powell, Marine applications of copper-nickel alloys, section 1: copper-nickel alloys-resistance to corrosion and biofouling, Tech. Rep. Copper Development Association, Potters Bar, United Kingdom, 1998.
- [5] F. Mansfeld, B.J. Little, Microbiologically influenced corrosion of copper based materials exposed to natural seawater, Electrochem. Acta 37 (1992) 2291-2297.
- [6] A. Hall, A.J.M. Baker, Settlement and growth of copper tolerant *Ectocarpus siliculosus* (Dillw.) Lyngbye on different copper-based antifouling surfaces under laboratory conditions, Mater. Sci. 20 (1985) 1111-1118.
- [7] C. Kato, B.G. Ateya, J.E. Castle, H.W. Pickering, On the mechanism of corrosion of Cu-9.4 Ni-1.7 Fe alloy in air saturated aqueous NaCl solution-I, Kinetic investigations, J. Electrochem. Soc. 127 (1980) 1890-1896.
- [8] S. Cere, M. Vazquez, Properties of the passive films present on copper and copper-nickel alloys in slightly alkaline solutions, J. Mater. Sci. Lett. 21 (2002) 493-495.
- [9] J.O.M. Bockris, B.T. Rubin, A. Despic, B. Lovrecek, The electro dissolution of copper nickel alloys, Electrochem. Acta 17 (1972) 973-999.
- [10] R.F. North, M.J. Pryor, The influence of corrosion product structure on the corrosion rate of Cu-Ni alloys, Corros. Sci. 10 (1970) 297-311.
- [11] Y.M. Kolotyrlkin, The electrochemistry of alloys, Electrochem. Acta 25 (1980) 89-96.
- [12] R. Walker, Aqueous corrosion of Tin-Bronze and inhibition by benzotriazole, Corros. 56 (2000) 1211-1219.
- [13] F. Mansfeld, M.W. Kending, S. Tsai, Determination of corrosion rates by electrochemical DC and AC methods, Corros. Sci. 21 (1981) 647-672.
- [14] M.M. Singh, R.B. Rastogi, B.N. Upadhyay, Thiosemicarbazide, phenyl isothiocyanate and their condensation product as corrosion inhibitors of copper in aqueous chloride solutions, Mater. Chem. Phys. 80 (2003) 283-293.
- [15] R. Ravichandran, N. Rajendran, Electrochemical behavior of brass in artificial sea water, Effect of organic inhibitors, Appl. Surf. Sci. 241 (2005) 449-458.
- [16] W.A. Badawy, K.M. Ismail, A.M. Fathi, Corrosion control of Cu-Ni alloys in neutral chloride solutions by amino acids, Electrochem. Acta. 59 (2006) 4182-4189.
- [17] M. Benmessaoud, K. Es-salah, N. Hajjaji, H. Takenouti, A. Srhiri, M. Ebentouhami, Inhibiting effect of 2-mercaptobenzimidazole on the corrosion of Cu-30Ni alloy in aerated 3% NaCl in presence of ammonia, Corros. Sci. 49 (2007) 3880-3888.
- [18] A. Frignani, L. Tommesani, C. Monticelli, G. Brunoro, M. Fogagnolo, Influence of the alkyl chain on the protective effects of 1,2,3-benzotriazole towards copper corrosion part I: inhibition of the anodic and cathodic reactions, Corros. Sci. 41 (1999) 1205-1215.

- [19] W. Qafsaoui, C. Blanc, J. Roques, N. Pebere, A. Shiri, et al, Pitting corrosion of copper in sulphate solutions: inhibitive effect of different triazole derivative inhibitors, *J. Appl. Electrochem.* 31 (2001) 223-231.
- [20] J. Shukla, K.S. Pitre, Electrochemical behavior of brass in acid solutions and the inhibitive effect of imidazole, *Corros. Rev.* 20 (2002) 217-228.
- [21] B. Mernari, H. El Attari, M. Traisnel, F. Bentiss, M. Lagrenee, Inhibiting effect of 3,5-Bis(N-Pyridyl)-4-amino-1,2,4-triazoles on the corrosion for mild steel in 1 M HCl medium, *Corros. Sci.* 40 (1998) 391-399.
- [22] S.S.A. El-Rehim, M.A.M. Ibrahim, 4-Aminoantipyrine as an inhibitor of mild steel corrosion in HCl solution, *J. Appl. Electrochem.* 29 (1999) 593-599.
- [23] F. Bentiss, M. Traisnel, M. Lagrenee, Inhibitor effects of triazole derivatives on corrosion of mild steel in acidic media, *Br. Corros. J.* 35 (2000) 315-320.
- [24] J.P. Ferreira, J.A. Rodrigues, I.T.E. Fonseca, Copper corrosion in buffered and non-buffered synthetic seawater: a comparative study, *J. Solid State Electrochem.* 8 (2004) 260-271.
- [25] L. Tang, G. Mu, G. Liu, The effect of 1-(2-pyridylazo)-2-naphthol on the corrosion of cold rolled steel in acid media: Part 2: inhibitive action in 0.5 M sulphuric acid, *Mater. Chem. Phys.* 97 (2006) 301-307.
- [26] L.M. Vracar, D.M. Drazic, Adsorption and corrosion inhibitive properties of some organic molecules on iron electrode in sulphuric acid, *Corros. Sci.* 44 (2002) 1669-1680.
- [27] S. Martinez, M. Metikoš-Hukovi, The inhibition of copper-nickel alloy corrosion under controlled hydrodynamic condition in seawater, *J. Appl. Electrochem.* 36 (2006) 1311-1315.